operative. The current result represents the lower limits of strength of the perovskite at these conditions.

We note that the pressure, temperature and stress levels in our experiment are not the same as the conditions in the Earth's lower mantle, where the temperature is probably 1,000 K higher and the stress level is about two orders of magnitude lower. Therefore the deformation mechanism probably falls into a different regime, and the current result can not be directly applied to the lower mantle. But this study reveals the rheological behaviour of $(Mg,Fe)SiO_3$ perovskite at high pressure and temperature, and suggests a revision of expectations that are based on room-temperature results[8]. It is probably more reasonable to predict the rheological behaviour of perovskite in the mantle from the present high-pressure and high-temperature experimental result, than from high-pressure but room-temperature data. Under the experimental conditions, using the data for both perovskite and ringwoodite (Fig. 1), we estimated the viscosity ($\eta = \sigma/\dot{\epsilon}$) of perovskite to be one order of magnitude higher than that of ringwoodite at 1,073 K. Once again, as the deformation in the Earth's lower mantle is likely to be dominated by diffusion creep, a more accurate comparison should be made on the basis of the diffusion creep data when they become available.

On the other hand, 1,073 K is a very reasonable temperature to be expected in subducted slabs at the bottom of the transition zone. Our experiment clearly shows that at this temperature perovskite is definitely much stronger than ringwoodite. This fact helps to explain why some subducted slabs deflect at top of the lower mantle, as the perovskite may create a mechanical barrier to subduction of the weaker ringwoodite[24]. Ultimately, the determination of the relative strengths of the different media must also consider other characteristics, such as grain-size effects as discussed by Karato *et al.*[25]. These authors showed that coarsening of the grain size increases the slab strength, and therefore a coarse-grained slab can penetrate into the lower mantle.

The mechanism of deep-focus earthquakes along subducted slabs has been a long-standing question, because the traditional brittle failure model is not likely to be operative in the deep mantle. With the progress in understanding the rheological properties of minerals, the early model of a thermal runaway instability[26,27]—when deformation of a material occurs so rapidly that heat is accumulated in the region of high strain—has regained special attention[25,28]. Using existing rheology data, Karato *et al.*[25] have modelled the rheological structure of subducted slabs in a fashion that satisfies the depth variation of seismicity down to the bottom of the transition zone. Lacking the rheology data for perovskite, these authors inferred that the clear shut-off of seismicity at the top of the lower mantle is probably attributable to loss of strength of the slabs in this depth region, owing to superplasticity and/or the absence of strong forces. In fact, following the thermal runaway instability model, thermal weakening (for example, the temperature-sensitive strength of olivine and ringwoodite[10]) enhances the positive feedback between deformation-induced heating and deformation. If the subducted slabs in the lower mantle consist of cold perovskite which does not weaken significantly with temperature as we observed (Fig. 1), the thermal runaway instability may not be promoted, with the result that earthquakes would not occur in the perovskite portion of the slab. □

Received 27 March; accepted 12 September 2002; doi:10.1038/nature01130.


1. Anderson, D. L. & Bass, J. D. Transition region of the Earth's upper mantle. *Nature* **320,** 321–328 (1986).
2. Poirier, J. P., Peyronneau, J., Gesland, J. Y. & Brebec, G. Viscosity and conductivity of the lower mantle: an experimental study on a $MgSiO_3$ perovskite analogue, $KZnF_3$. *Phys. Earth Planet. Inter.* **32,** 273–287 (1983).
3. Doukhan, N. & Doukhan, J. C. Dislocation in perovskite $BaTiO_3$ and $CaTiO_3$. *Phys. Chem. Miner.* **13,** 403–410 (1986).
4. Karato, S.-i. Plasticity-crystal structure systematics in dense oxides and its implications for the creep strength of the Earth's deep interior: a preliminary result. *Phys. Earth Planet. Inter.* **55,** 234–240 (1989).
5. Karato, S.-i. & Li, P. Diffusion creep in perovskite: implications for the rheology of the lower mantle. *Science* **255,** 1238–1240 (1992).
6. Li, P., Karato, S.-i. & Wang, Z. High-temperature creep in fine-grained polycrystalline $CaTiO_3$, an analogue material of $(Mg,Fe)SiO_3$ perovskite. *Phys. Earth Planet. Inter.* **95,** 19–36 (1996).
7. Wright, K., Price, G. D. & Poirier, J. P. High-temperature creep of the perovskite $CaTiO_3$ and $NaNbO_3$. *Phys. Earth Planet. Inter.* **74,** 9–22 (1992).
8. Meade, C. & Jeanloz, R. The strength of mantle silicates at high pressures and room temperature: implications for the viscosity of the mantle. *Nature* **348,** 533–535 (1990).
9. Karato, S.-i., Fujino, K. & Ito, E. Plasticity of $MgSiO_3$ perovskite: the results of microhardness tests on single crystals. *Geophys. Res. Lett.* **17,** 13–16 (1990).
10. Chen, J., Inoue, T., Weidner, D., Wu, Y. & Vaughan, M. Strength and water weakening of mantle minerals, olivine, wadsleyite and ringwoodite. *Geophys. Res. Lett.* **25,** 575–578 1103–1104 (1998).
11. Weidner, D. J., *et al. High-pressure Research: Application to Earth and Planetary Sciences* (eds Syono, Y. & Manghnani, M. H.) 13–17 (Terra Scientific/AGU, Tokyo/Washington DC, 1992).
12. Weidner, D. J., Wang, Y. & Vaughan, M. T. Yield strength at high pressure and temperature. *Geophys. Res. Lett.* **21,** 753–756 (1994).
13. Weidner, D. J., Wang, Y., Chen, G., Ando, J. & Vaughan, M. T. *Properties of Earth and Planetary Materials at High Pressure and Temperature* (eds Manghnani, M. H. & Yagi, T.) 473–482 (Geophysical Monograph, AGU, Washington DC, 1998).
14. Decker, D. L. High-pressure equation of state for NaCl, KCl and CsCl. *J. Appl. Phys.* **42,** 3239–3244 (1971).
15. Gerward, L., Morup, S. & Topsoe, H. Particle size and strain broadening in energy-dispersive x-ray powder patterns. *J. Appl. Phys.* **47,** 822–825 (1976).
16. Frost, H. J. & Ashby, M. F. *Deformation-Mechanism Maps* (Pergamon, Oxford, 1982).
17. Wang, Y., Guyot, F., Yeganeh-Haeri, A. & Liebermann, R. C. Twinning in $MgSiO_3$ perovskite. *Science* **248,** 468–471 (1990).
18. Sapriel, J. Domain-wall orientations in ferroelastics. *Phys. Rev. B* **12,** 5128–5140 (1975).
19. Toledano, J. C. & Toledano, P. Order parameter symmetries and free-energy expansions for purely ferroelastic transitions. *Phys. Rev. B* **21,** 1139–1172 (1980).
20. Zhao, Y. *et al.* High-pressure crystal chemistry of neighborite, $NaMgF_3$: An angle-dispersive diffraction study using monochromatic synchrotron x-radiation. *Am. Mineral.* **79,** 615–621 (1994).
21. Avé Lallemant, H. G. Experimental deformation of diopside and websterite. *Tectonophysics* **48,** 1–27 (1978).
22. Derby, B. *Deformation Processes in Minerals, Ceramics and Rocks* (eds Barber, D. J. and Meredith, P. G.) 354–364 (Unwin Hyman, London, 1990).
23. Shimuzu, I. Stress and temperature dependence of recrystallized grain size: A subgrain misorientation model. *Geophys. Res. Lett.* **25,** 4237–4240 (1998).
24. Gurnis, M. & Hager, B. H. Controls of the structure of subducted slabs. *Nature* **335,** 317–321 (1988).
25. Karato, S.-i., Riedel, M. R. & Yuen, D. A. Rheological structure and deformation of subducted slabs in the mantle transition zone; implications for mantle circulation and deep earthquakes. *Physics Earth Planet. Inter.* **127,** 83–108 (2001).
26. Griggs, D. T. & Baker, D. W. *Properties of Matter Under Unusual Conditions* (eds Mark, H. & Fernbach, S.) 23–42 (Wiley/Interscience, New York, 1969).
27. Ogawa, M. Shear instability in a viscoelastic material as the cause of deep focus earthquakes. *J. Geophys. Res.* **92,** 13801–13810 (1987).
28. Weidner, D. J. *et al.* Subduction zone rheology. *Phys. Earth Planet. Inter.* **127,** 67–81 (2001).


**Acknowledgements** This work was carried out at the X17B beamline of the National Synchrotron Light Source. We thank Z. Zhang, J. B. Hastings and D. P. Siddons for technical support at the beamline, and J. Zhang for help in sample preparation. This work was supported by the US National Science Foundation.

**Competing interests statement** The authors declare that they have no competing financial interests.

**Correspondence** and requests for materials should be addressed to J.C. (e-mail: jiuhua.chen@sunysb.edu).

# Contemporary fisherian life-history evolution in small salmonid populations

**Mikko T. Koskinen*, Thrond O. Haugen† & Craig R. Primmer***

** Department of Ecology and Systematics, Division of Population Biology, PO Box 65, Viikinkaari 1, FIN-00014, University of Helsinki, Finland*
*† Department of Biology, Division of Zoology, PO Box 1050, Blindern, N-0316, Oslo, Norway*

**The relative importance of natural selection[1] and random drift[2] in phenotypic evolution has been discussed since the introduction of the first population genetic models[3–5]. The empirical evidence used to evaluate the evolutionary theories of Fisher[1] and Wright[2] remains obscure because formal tests for neutral divergence[6–8] or sensitive attempts to separate the effects of**

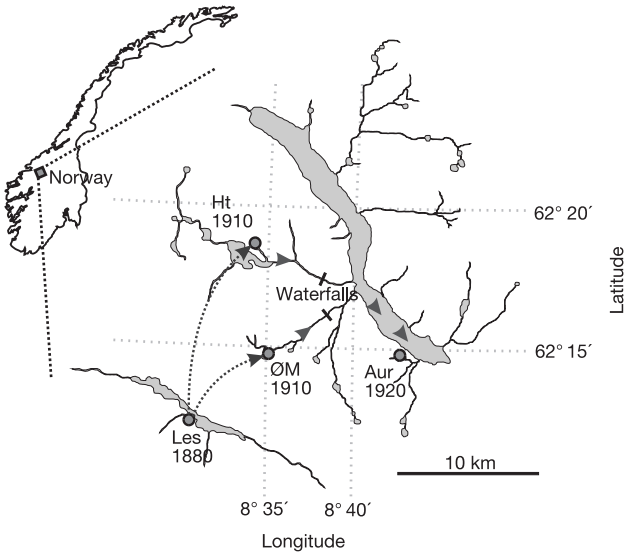


**Figure 1** Map presenting the study region and location of the *T. thymallus* populations. The population in Lake Lesjaskogsvatn (Les) was founded in 1880 and used for introducing a small number of grayling into lakes Hårrtjønn (Ht) and Øvre Mærrabottvatn (ØM) in 1910. These populations were the sources for colonization of Aursjøen (Aur), where grayling were first observed in 1920. All grayling in the system originate from these introductions. Land or impassable waterfalls prevent all migration between Les–Ht, Les–ØM, Les–Aur and Ht–ØM.

**selection and drift are scarce, subject to error, and have not been interpreted in the light of well-known population demography. We combined quantitative genetic and microsatellite DNA analyses to investigate the determinants of contemporary life-history evolution in isolated populations of grayling (*Thymallus thymallus*, Salmonidae) that originated from a common source 80–120 years ago. Here we show that natural selection was the dominant diversifying agent in the evolution of the quantitative traits. However, the populations were founded by a small number of individuals, exhibit very low microsatellite-based effective sizes and show genetic imprints of severe 'bottlenecks'; which are conditions often suggested to constrain selection and favour drift[6,8,9]. This study demonstrates a very clear case of fisherian evolution in small natural populations across a contemporary timescale.**

The fisherian view of evolution holds that phenotypic differentiation results primarily from positive natural selection[1]. In contrast, the influential theories developed by Wright[2] and evolutionists working after Wright[6,8,9] emphasize the potential importance of random drift in effectively small populations. Evidence from species experiencing changing environmental conditions suggest that directional selection can be powerful in nature[10–14]. However, the evolutionary theories warrant further study for several reasons.

First, formal tests for the null-hypothesis of neutral evolution[6–8] have rarely been applied to wild organisms[8,15]. This is because the tests require knowledge of mutational input, divergence time ($t$) and effective population size ($N_e$), which are normally unknown or subject to considerable error[5]. Second, despite the published examples of natural selection[10–14], sensitive attempts to evaluate the potential effect of drift in phenotypic evolution remain scarce. A promising indirect method is to compare genetic differentiation based on quantitative traits ($Q_{ST}$)[16] and DNA markers affected by drift ($F_{ST}$)[17]. Third, studies applying the neutrality tests[8,15] or attempting to separate the causes of evolution[16] were performed for populations that diverged thousands of generations ago, leaving much room for error owing to migration from unknown sources, differing mutational contribution on coding genes and neutral markers, or convergence of $F_{ST}$ on its maximal value[5]. Thus, although these two important methods of evolutionary inference are most useful across contemporary timescales, such applications have not been reported. Finally, studies linking the relative importance of selection and drift with well-known population demography are nonexistent. This is a major caveat for evaluation of the evolutionary theories because many models consider $N_e$ as the key parameter expected to influence the power of the alternative diversifying agents[6,8,9].

Here we present an investigation in an exceptional natural model system that provides a sensitive framework for assessing the relative importance of selection and drift on quantitative trait divergence. Importantly, this study effectively avoids the above-mentioned sources of bias and involves populations with well-known demographic histories, providing an unequivocal evaluation of the

Table 1 **Evidence for natural selection**

| Trait | Pairwise comparison | $h^2$ | $s'$ | $\sigma^2_{GW}$ | $\sigma^2_{GB}$ | $F_{1,\infty}$ | $P$ | $N_e$(sign) |
|---|---|---|---|---|---|---|---|---|
| Length at termination (mm) | Les–Ht | 0.10 | 0.95 | 0.08 | 1.47 | 384 | *** | 0.25 |
| | Les–Aur | 0.06 | 0.58 | 0.18 | 0.03 | 10.7 | * | 22.6 |
| | Ht–Aur | 0.06 | 1.07 | 0.27 | 0.72 | 134 | *** | 0.93 |
| Yolk-sac volume (mm$^3$) | Les–Ht | 0.05 | 1.73 | 0.17 | 2.40 | 647 | *** | 0.14 |
| | Les–Aur | 0.03 | 3.24 | 0.44 | 5.55 | $1.78\times10^3$ | *** | 0.12 |
| | Ht–Aur | 0.03 | 2.07 | 0.46 | 0.45 | 99.3 | *** | 1.54 |
| Growth rate (mm/Δ$D$) | Les–Ht | 0.18 | 0.41 | $6.57\times10^{-5}$ | $6.55\times10^{-4}$ | 111 | *** | 0.84 |
| | Les–Aur | 0.22 | 0.21 | $7.23\times10^{-5}$ | $9.72\times10^{-5}$ | 28.2 | *** | 7.54 |
| | Ht–Aur | 0.22 | 0.42 | $1.73\times10^{-5}$ | $2.22\times10^{-4}$ | 194 | *** | 0.79 |
| Survival (%) | Les–Ht | 0.09 | 0.66 | 0.08 | 0.23 | 65.7 | *** | 1.42 |
| | Les–Aur | 0.13 | 0.32 | 0.12 | 0.08 | 22.0 | *** | 8.84 |
| | Ht–Aur | 0.13 | 0.38 | 0.27 | 0.10 | 9.43 | * | 16.6 |
| Incubation time (days) | Les–Ht | 0.22 | 0.26 | 0.26 | 0.50 | 17.4 | ** | 5.33 |
| | Les–Aur | 0.44 | 0.04 | 0.30 | $1.00\times10^8$ | $3.45\times10^{-7}$ | >0.99 | $6.16\times10^8$ |
| | Ht–Aur | 0.44 | 0.13 | 0.24 | 0.58 | 18.0 | ** | 8.49 |
| Swim-up length (mm) | Les–Ht | 0.11 | 0.72 | 0.02 | $2.50\times10^{-3}$ | 2.50 | 0.12 | 37.1 |
| | Les–Aur | 0.32 | 0.03 | 0.04 | $3.13\times10^{-4}$ | 0.12 | 0.73 | $1.73\times10^3$ |
| | Ht–Aur | 0.32 | 0.22 | 0.11 | $9.28\times10^{-10}$ | $8.32\times10^{-8}$ | >0.99 | $1.83\times10^9$ |
| Hatching length (mm) | Les–Ht | 0.15 | 0.38 | 0.51 | $3.62\times10^{-9}$ | $9.53\times10^{-8}$ | >0.99 | $9.76\times10^8$ |
| | Les–Aur | 0.08 | 0.53 | 0.27 | $2.37\times10^{-9}$ | $4.84\times10^{-7}$ | >0.99 | $4.40\times10^8$ |
| | Ht–Aur | 0.08 | 1.11 | 0.03 | $6.09\times10^{-4}$ | 0.70 | 0.40 | 218 |

$h^2$ is the narrow-sense heritability for the youngest population in each comparison. The standardized selection differentials ($s'$) indicating the strength of directional selection (in s.d. units per generation), were obtained from the ratio of haldane estimates[18] and the corresponding $h^2$ estimates[24]. $\sigma^2_{GW}$, Additive genetic variance within populations; $\sigma^2_{GB}$, Additive genetic variance between populations. $F = (N_e\sigma^2_{GB})/(h^2\sigma^2_{GW}t)$ (refs 6, 7), where $N_e$ is the maximum likelihood estimate of effective population size (Table 2; Supplementary Information), and $t$ equals 11.8, 11.8 and 12.3 generations between Les–Ht, Les–Aur and Ht–Aur, respectively. The $P$-values have been adjusted for multiple significance tests using a Bonferroni correction. ***, $P < 0.0001$; **, $0.0001 \le P < 0.001$; *, $0.001 \le P < 0.01$. $N_e$ (sign) is the level of effective population size required to produce an $F$-value leading to rejection of the null-hypothesis at the $P \le 0.05$ significance level ($F_{1,\infty} = 3.84$).


© 2002 Nature Publishing Group

determinants of phenotypic evolution.

Grayling inhabiting Lake Lesjaskogsvatn (Les), Norway, originate from a single human-mediated introduction in 1880 (Fig. 1). Thirty years later, a local fisherman carried a small number of individuals from Lesjaskogsvatn into two nearby mountain lakes, Hårrtjønn (Ht) and Øvre Mærrabottvatn (ØM). The exact number of individuals in the fisherman's bucket remains unknown, but was very small because Ht and ØM are separated from Les by approximately five hours of demanding uphill hiking, making it impossible for the fisherman to transfer large volumes of water (J. Nordsletten, personal communication). The founders of Ht and ØM (or their offspring) subsequently dispersed downstream into Aursjøen (Aur), where grayling were first observed in 1920 (Fig. 1). All *T. thymallus* in the system (Fig. 1) are well known to originate from these stocking and dispersal events (J. Nordsletten, personal communication). When the divergence times of the populations are combined with their generation intervals in Les, Ht, ØM and Aur (4.0–7.5 yr, as estimated using the 'life table method' that accounts for overlapping generations[18]), it follows that the populations coalesce to a common ancestor 11.8–22.0 generations ago. With so few generations, diversifying mutations are negligible causes of phenotypic differentiation (see discussion in ref. 19). Further, migration to three of the populations has been impossible since their founding, either due to barriers formed by land (Les; Fig. 1) or impassable waterfalls (Ht and ØM; Fig. 1).

The null-hypothesis of neutral evolution was tested[6,7] for divergence of seven life-history traits obtained from a 'common-garden' experiment. The null-hypothesis was rejected for the majority of the quantitative traits with a very high level of confidence ($F_{1,\infty}$; $P < 0.0001$; Table 1). Evidence against divergence at a neutral rate was compelling in all of the pairwise population comparisons for length at temination, yolk-sac volume, growth rate and survival (Table 1). For these traits, the additive genetic interpopulation differences were so large that unrealistically small $N_e$ estimates would have been necessary for evolution to proceed due to drift alone (Table 1). For instance, neutral divergence of yolk-sac volume would have required an average $N_e$ of only 0.12–1.54 individuals (mean across populations, 0.60) throughout the evolutionary time periods of the grayling populations (Table 1). Such small theoretical estimates exclude drift as being the dominant evolutionary process. Strength of selection was estimated also using standardized selection differentials ($s'$). These estimates revealed that most traits had been under very strong directional selection pressure: the mean selection differentials across traits (among populations) were 0.71–0.77 (Table 1), which are above the 96th percentile of the estimates normally observed in natural populations[20].

We compared among-population differences based on additive genetic variances from the common-garden experiment ($Q_{ST}$[16]) and analogous measures based on microsatellite DNA from analysis of 17 loci ($F_{ST}$[17]; microsatellite allele frequencies are available in the Supplementary Information). This is a well-established indirect method for separating the causes of adaptive divergence[16]. Well in line with the neutrality test results, the quantitative trait divergence often greatly exceeded the microsatellite divergence (Fig. 2). Hence, evolution of many of the traits was driven by divergent natural selection instead of random drift. For instance, the pairwise $Q_{ST}$ estimates for growth rate (0.36–0.88) were 4–10 times higher than the corresponding $F_{ST}$ estimates (Fig. 2). Importantly, our $Q_{ST}/F_{ST}$ comparisons are not biased by phenotypic plasticity (genetic variances were obtained from a common-garden experiment), maternal effects (sire components of additive genetic variances were used for the $Q_{ST}$ estimation[19]), or mutations (owing to the short coalescence times), factors which have commonly been a potential source for error[5]. We have assumed that physical linkages between the microsatellites and genes determining the life-history evolution are not biasing the $Q_{ST}/F_{ST}$ comparisons. Such linkages, however, would only make our conclusions regarding the dominating effect of selection conservative: divergent selective sweeps to microsatellite allele frequencies would increase the $F_{ST}$ estimates.

We note that all of the life-history traits included in this study are very important for fitness of *T. thymallus*[21] and that many of the traits evolved primarily owing to directional selection (Table 1; Fig. 2). When offspring of the populations were reared in the three distinct July–August water temperatures naturally occurring within Lesjaskogsvatn, Hårrtjønn and Aursjøen, they performed best in the experimental temperatures that corresponded precisely with the natural conditions[21]. For instance, grayling originating from the naturally warm Lake Hårrtjønn exhibited the highest survival rate in warm experimental conditions (and lowest survival in cold conditions), whereas individuals from the naturally cold Lake Aursjøen exhibited highest survival in a cold environment (and lowest survival in warm conditions). Accordingly, grayling originating from Lesjaskogsvatn, a lake with medium natural temperatures, exhibited highest survival rates in medium temperature conditions[21]. This population × temperature interaction effect was highly significant ($F_{4,148} = 6.53$, $P < 0.0001$)[21]. It therefore seems very likely that selection acted in favour of local adaptation to the specific temperatures that the populations experience in nature.

The fisherian view of evolution[1] has often been challenged by

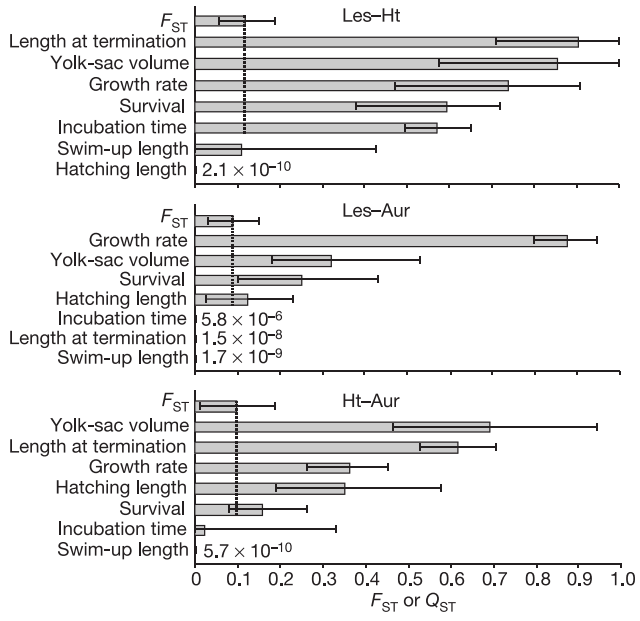


**Figure 2** Among-population genetic differences based on additive genetic variances of seven life-history traits ($Q_{ST}$), and analogous measures based on 17 microsatellite DNA loci ($F_{ST}$). The horizontal bars indicate 95% confidence intervals for the $F_{ST}$ and $Q_{ST}$ estimates. Combined effects of natural selection and random drift determine the $Q_{ST}$ estimates, whereas the $F_{ST}$ estimates are determined by drift processes[16]. The dashed vertical bars indicate the effect of drift (left-hand side) and selection (right-hand side) on the quantitative traits that have been influenced by divergent selection.

Table 2 **Genetic diversity and demography of populations**

| | *n* | *A* (s.d.) | $H_o$ (s.d.) | $N_e$ (95% CI) | $N_0/N_1$ (95% CI) |
|---|---|---|---|---|---|
| Les | 52 | 1.9 (±1.1) | 0.17 (±0.23) | 88.9* | 0.003 (0.0003–0.03) |
| Ht | 48 | 1.5 (±0.9) | 0.14 (±0.25) | 24.2 (12.1–42.2) | 0.006 (0.0003–0.05) |
| ØM | 49 | 1.7 (±0.9) | 0.17 (±0.24) | 85.0 (36.0–170.5) | 0.0006 (0.00008–0.01) |
| Aur | 28 | 1.6 (±0.9) | 0.14 (±0.20) | 55.4 (24.8–110.0) | 0.001 (0.0003–0.005) |

*A* is the mean allele number within populations. $H_o$ is the mean observed heterozygosity within populations.
*Indicates the lowest sampled point of effective population size ($N_e$) out of 100,000 MCMC replicates. The maximum likelihood estimate of $N_e$ could not be obtained, most probably owing to near-zero level of drift in the Les population (M. A. Beaumont, personal communication). $N_0/N_1$ is the ratio of current population size ($N_0$) and historical population size ($N_1$; Supplementary Information)[29].


© 2002 Nature Publishing Group

models emphasizing the importance of drift in small or bottlenecked populations[2,6,8,9]. Our results are especially pertinent to this discussion (at the phenotypic level of adaptive differentiation) because: (1) the effect of drift is also estimated; and (2) the results are considered in the light of population demography. That selection often clearly outweighed drift is striking because the *T. thymallus* populations originated from a small number of founders, and were thus predisposed to the influence of drift[2,6,8,9]. In line with the known demographic history, we also found that the populations exhibit very small microsatellite-based $N_e$ estimates and show signatures of severe bottlenecks (Table 2). The low effective population sizes and bottlenecks were exemplified by the Hårrtjønn grayling which had an average of only 1.5 (s.d., ±0.9) alleles per locus ($A$), a harmonic mean $N_e$ of 24.2 (95% confidence interval (CI) = 12.1–42.2) individuals since the founding of the population and a current population size of 0.6% (95% CI = 0.03–5%) of its historical size (Table 2). As a comparison, *T. thymallus* populations are generally much more diverse, exhibiting an average of 4.0 (s.d., ±0.8) alleles per locus, as revealed using the same set of microsatellites[22]. Although the estimated effective sizes are low for natural salmonid populations, they seem to be realistic because of the small ecological niches characterizing the Norwegian mountain lakes investigated. For instance, the total area of Hårrtjønn is only 0.35 $km^2$ and the lake has a single 10 $m^2$ *T. thymallus* spawning ground, thus providing a suitable habitat for only a very small reproducing population.

Evolutionary models commonly predict notable divergence owing to random drift in effectively small populations[2,6,8,9]. In this study, microsatellites indeed revealed highly significant ($P < 0.001$) genetic differentiation between all of the populations and pairwise $F_{ST}$ estimates from 0.05 (95% CI = 0.01–0.09) to 0.21 (95% CI = 0.10–0.34; Fig. 2; Supplementary Information). Because divergence was evident at multiple loci (Supplementary Information), it is highly unlikely that the $F_{ST}$ estimates were solely due to physical linkages to genes under selection. We therefore conclude that, although the populations evolved dominantly due to selection, drift had an effect on the quantitative trait divergence.

Are such high levels of drift theoretically feasible with constant $N_e$, or must founder events, fluctuating population sizes, or even selection be invoked to explain the $F_{ST}$estimates? We used computer simulated genotypes to address this question. When applying the known coalescence times and the microsatellite-based $N_e$ estimates, it was evident that the empirically obtained $F_{ST}$ estimates were theoretically expected, even though the populations shared common ancestors as few as 11.8 generations ago (Supplementary Information). In other words, the effective population sizes were sufficiently low to generate the observed levels of neutral divergence, even without variation in the number of breeders (or selection) throughout the independent evolutionary histories of the grayling populations (Supplementary Information).

Thus we have shown that selection was the dominant diversifying mechanism during the early stages of grayling life-history evolution. The power of natural selection is striking because the populations originate from a small number of founders, exhibit small effective sizes and show genetic imprints of bottlenecks, which are all conditions expected to constrain selection and favour the influence of drift[2,6,8,9]. This study demonstrates a very clear case of fisherian evolution across a contemporary timescale. □

## Methods

### Population differences based on quantitative traits

The seven early life-history traits studied were: (1) incubation time (number of days from fertilization to hatching); (2) fork length (length from the tip of the snout to the tip of the median rays of the tail in mm) at hatching; (3) yolk-sac volume in $mm^3$ (estimated as $L_{YS}H_{YS}^2(\pi/6)$, where $L_{YS}$ and $H_{YS}$ are the length and height of yolk-sac in mm, respectively); (4) fork length at swim-up ($L_{SU}$; measured when yolk-sac is resorbed and an individual begins exogenous feeding); (5) fork length at termination ($L_{term}$), measured at 180 degree-days ($\Delta D$ = mean temperature in °C × number of days); (6) specific growth rate (mm/$\Delta D$) $G = 100[(\ln L_{term} - \ln L_{SU})/\Delta D]$; and (7) survival (%) during 180 degree-days of exogenous feeding.

The level of quantitative genetic differentiation ($Q_{ST}$) was estimated as follows: $Q_{ST} = \sigma^2_{GB}/(\sigma^2_{GB} + 2\sigma^2_{GW})$, where $\sigma^2_{GB}$ and $\sigma^2_{GW}$ are additive genetic variances between and within populations, respectively[16]. Restricted maximum likelihood (REML) estimates of $\sigma^2_{GB}$ and $\sigma^2_{GW}$ were obtained with programs S-PLUS 6.0 and SAS 8.0 from a common-garden experiment using a hierarchical half-sib design, where each male was mated with four unique females, yielding up to 28 families per population. The experiment involved three temperatures, mimicking the natural nursery conditions for the three populations involved[21]. Consequently, $\sigma^2_{GB}$ and $\sigma^2_{GW}$ were extracted from a nested mixed-model analysis of variance (ANOVA) as recommended[23]. Population, male and female were treated as random effects, and temperature, temperature × population and temperature × male as fixed effects. In order to avoid non-genetic maternal sources of variance, the $\sigma^2_{GW}$ estimates were derived from the male variance component only. The $\sigma^2_{GW}$ estimates were multiplied with four to take into account the half-sib design.

A two-model ANOVA approach[18] was used to test whether maternal effects (egg size) significantly contributed to among-population divergence. No evidence for among-population maternal effects was obtained ($F_{2,4} = 0.002–0.924, P > 0.5$). Non-parametric bootstrapping at the family level was used to assess 95% confidence intervals for the $Q_{ST}$ estimates. The strength of directional selection was estimated using the standardized selection differentials ($s'$; in s.d. units per generation) obtained from the ratio of the trait- and environment-specific haldane estimates[18] and the corresponding narrow-sense heritability estimates ($h^2$; ref. 24). The narrow-sense heritability was estimated from $4\sigma^2_A/\sigma^2_P$, where $\sigma^2_A$ is the population and temperature-specific additive genetic variance (male component of variance) and $\sigma^2_P$ is the corresponding total phenotypic variance derived from nested ANOVAs (REML method[21]).

### Microsatellite analyses

Spawning grayling were sampled between the years 1995 and 2000. The individuals were genotyped with 17 microsatellite loci applying previously described protocols[25]. All of the loci are highly variable in *T. thymallus*[22]. Deviations from Hardy–Weinberg equilibrium and linkage equilibrium were tested for each population and locus using the exact probability tests implemented in computer program GENEPOP 3.2a[26]. No deviations were observed, even if the $P$-values were not adjusted for multiple significance tests. Estimates of interpopulation differentiation ($F_{ST}$)[17] and their 95% confidence intervals were obtained using the variance component approach (providing the $F_{ST}$ estimator theta[26]) and bootstrapping of loci with program FSTAT 2.9.3.1[27].

Harmonic mean effective sizes of the populations ($N_e$) were estimated using a coalescent theory maximum likelihood approach that uses a Metropolis–Hastings algorithm to estimate the range of $N_e$ values consistent with the data (Supplementary Information)[28]. Past variation in the sizes of the populations was estimated using a Markov Chain Monte Carlo (MCMC) simulation method[29]. The approach assesses the most probable demographic histories of populations using the estimator $r = N_0/N_1$, where $N_0$ and $N_1$ are present and past population sizes, respectively (Supplementary Information)[29]. Computer simulations were used to assess theoretically expected $F_{ST}$ values with the known coalescence times, and the maximum likelihood estimates and the 95% confidence intervals of effective population sizes (Supplementary Information)[30].

### Causes of phenotypic microevolution

The null-hypothesis of evolution by random drift was tested as follows: $F = (N_e\sigma^2_{GB})/(h^2\sigma^2_{GW}t)$, where $N_e$ is the maximum likelihood estimate of effective population size and $h^2$ the narrow-sense heritability of a trait in a given population and environment[6,7]. The numerator and denominator degrees of freedom are the number of populations compared minus one; and infinity, respectively[7]. We applied the mean of the maximum likelihood $N_e$ estimates of Ht and Aur when testing for neutrality of their divergence. A maximum likelihood estimate of $N_e$ could not be obtained for the Les population, and the $N_e$ of Ht or Aur was applied when testing for neutrality of the evolution of Les–Ht and Les–Aur, respectively. Because the instability of the Metropolis–Hastings sampler was most probably due to a near-zero level of drift in the Les population (M. A. Beaumont, personal communication), the neutrality test results involving Les are conservative. The neutrality test equation[7] was also applied to estimate the extent of $N_e$ required to produce an $F$-value leading to rejection of the null-hypothesis at the $P \leq 0.05$ significance level ($F_{1,\infty} = 3.84$). Population differences based on analogous measures obtained from quantitative traits ($Q_{ST}$) and microsatellites ($F_{ST}$) were compared[16]. Neutral divergence of quantitative traits will result in equal estimates of $Q_{ST}$ and $F_{ST}$. The magnitude of differences between $Q_{ST}$ and $F_{ST}$ can be used to infer the relative contribution of selection and drift on phenotypic divergence[16].

Received 13 June; accepted 11 July 2002; doi:10.1038/nature01029.

1. Fisher, R. A. *The Genetical Theory of Natural Selection* (Oxford Univ. Press, Oxford, 1930).
2. Wright, S. Evolution in mendelian populations. *Genetics* **16,** 97–159 (1931).
3. Kimura, M. *The Neutral Theory of Molecular Evolution* (Cambridge Univ. Press, Cambridge, 1983).
4. Gillespie, J. H. *The Causes of Molecular Evolution* (Oxford Univ. Press, Oxford, 1991).
5. Schluter, D. *The Ecology of Adaptive Radiation* (Oxford Univ. Press, Oxford, 2000).
6. Lande, R. Natural selection and random genetic drift in phenotypic evolution. *Evolution* **30,** 314–334 (1976).
7. Lande, R. Statistical tests for natural selection on quantitative characters. *Evolution* **31,** 442–444 (1977).
8. Lynch, M. The rate of morphological evolution in mammals from the standpoint of the neutral expectation. *Am. Nat.* **136,** 727–741 (1990).
9. Carson, H. L. & Templeton, A. R. Genetic revolutions in relation to speciation phenomena: the founding of new populations. *Annu. Rev. Ecol. Syst.* **15,** 97–131 (1984).
10. Losos, J. B., Warheit, K. I. & Schoener, T. W. Adaptive differentiation following experimental island colonization in *Anolis* lizards. *Nature* **387,** 70–73 (1997).


© 2002 Nature Publishing Group

11. Reznick, D. N., Shaw, F. H., Rodd, F. H. & Shaw, R. G. Evaluation of the rate of evolution in natural populations of guppies (*Poecilia reticulata*). *Science* **275,** 1934–1936 (1997).
12. Majerus, M. E. N. *Melanism: Evolution in Action* (Oxford Univ. Press, Oxford, 1998).
13. Hendry, A. P. Adaptive divergence and the evolution of reproductive isolation in the wild: an empirical demonstration using introduced sockeye salmon. *Genetica* **112,** 515–534 (2001).
14. Grant, P. R. & Grant, B. R. Unpredictable evolution in a 30-year study of Darwin's finches. *Science* **296,** 707–711 (2002).
15. Baker, A. J. Genetic and morphometric divergence in ancestral European and descendent New Zeland populations of chaffinches (*Fringilla coelebs*). *Evolution* **46,** 1784–1800 (1992).
16. Merilä, J. & Crnokrak, P. Comparison of genetic differentiation at marker loci and quantitative traits. *J. Evol. Biol.* **14,** 892–903 (2001).
17. Wright, S. The genetical structure of populations. *Ann. Eugen.* **15,** 323–354 (1951).
18. Haugen, T. O. & Vøllestad, L. A. A century of life-history evolution in grayling. *Genetica* **112,** 475–491 (2001).
19. Lynch, M. & Walsh, B. *Genetics and Analysis of Quantitative Traits* 328–352 (Sinauer, Sunderland, 1998).
20. Kingsolver, J. G. *et al.* The strength of phenotypic selection in natural populations. *Am. Nat.* **157,** 245–261 (2001).
21. Haugen, T. O. & Vøllestad, L. A. Population differences in early life-history traits in grayling. *J. Evol. Biol.* **13,** 897–905 (2000).
22. Koskinen, M. T. *et al.* Microsatellite data resolve phylogeographic patterns in European grayling, *Thymallus thymallus*, Salmonidae. *Heredity* **88,** 391–401 (2002).
23. Fry, J. D. The mixed-model analysis of variance applied to quantitative genetics: biological meaning of the parameters. *Evolution* **46,** 540–550 (1992).
24. Hendry, A. P. & Kinnison, M. T. The pace of modern life: measuring rates of contemporary microevolution. *Evolution* **53,** 1637–1653 (1999).
25. Koskinen, M. T. & Primmer, C. R. High throughput analysis of 17 microsatellite loci in grayling (*Thymallus* spp. Salmonidae). *Conserv. Genet.* **2,** 173–177 (2001).
26. Raymond, M. & Rousset, F. GENEPOP (version 1.2): population genetics software for exact tests and ecumenicism. *J. Hered.* **86,** 248–249.
27. Goudet, J. FSTAT (vers. 1.2): a computer program to calculate F-statistics. *J. Hered.* **86,** 485–486 (1995).
28. O'Ryan, C. *et al.* Microsatellite analysis of genetic diversity in fragmented South African buffalo populations. *Anim. Conserv.* **1,** 85–94 (1998).
29. Beaumont, M. A. Detecting population expansion and decline using microsatellites. *Genetics* **153,** 2013–2029 (1999).
30. Balloux, F. EASYPOP (version 1.7): a computer program for population genetics simulations. *J. Hered.* **92,** 301–302 (2001).


**Supplementary Information** accompanies the paper on *Nature*'s website (http://www.nature.com/nature).


**Acknowledgements** We thank A. Hendry for his thorough reviews. We also thank M. Beaumont, P. Bredbacka, P. Crnokrak, D. Johnson, M. Lascoux, J. Merilä, R. O'Hara, W. Provine, N. Smith and A. Vøllestad for comments. The work was supported by grants from the Biological Interactions Graduate School, University of Helsinki and the Finnish Academy.

**Competing interests statement** The authors declare that they have no competing financial interests.



**Correspondence** and requests for materials should be addressed to M.T.K. (e-mail: mtkoskin@cc.helsinki.fi).


# Paternal inheritance of a female moth's mating preference


**Vikram K. Iyengar, H. Kern Reeve & Thomas Eisner**

*Department of Neurobiology and Behavior, Cornell University, Ithaca, New York 14850, USA*



**Females of the arctiid moth *Utetheisa ornatrix* mate preferentially with larger males, receiving both direct phenotypic and indirect genetic benefits[1]. Here we demonstrate that the female's mating preference is inherited through the father rather than the mother, indicating that the preference gene or genes lie mostly or exclusively on the Z sex chromosome, which is strictly paternally inherited by daughters. Furthermore, we show that the preferred male trait and the female preference for that trait are correlated, as females with larger fathers have a stronger preference for larger males. These findings are predicted by the protected invasion theory[2,3], which asserts that male homogametic sex chromosome systems (ZZ/ZW) found in lepidopterans and birds promote the evolution of exaggerated male traits through sexual selection. Specifically, the theory predicts that, because female preference alleles arising on the Z chromosome are transmitted to all sons that have the father's attractive trait rather than to only a fraction of the sons, such alleles will experience stronger positive selection and be less vulnerable to chance loss than would autosomal alleles.**


The benefits accrued by female *Utetheisa* as a result of mating preferentially with larger males have been characterized. The phenotypic benefits take the form of nutrient and pyrrolizidine alkaloid transmitted seminally by the male to the female in quantities proportional to his size[4–6]. The nutrient enables the female to increase her egg production[7], and the alkaloid bestows chemical protection upon herself[8] and her eggs[1,5]. The genetic benefits, realized as a consequence of the heritability of body size[9], ensure that females, by choosing larger males, have larger sons which are themselves more likely to be favoured in courtship, and larger daughters bound to be more fecund[1]. The cumulative effect of these benefits is substantial: a female given a choice between males differing by 10% in body mass will have an estimated 25% more grandchildren by mating with the larger male. The strong selection for large males in *Utetheisa* may account for why in this species, contrary to the norm for Lepidoptera[10], males are larger than females[11].

Sexual selection models generally assume heritable variation in both the trait and the mating preference, and a genetic correlation between trait and preference[12,13]. In *Utetheisa*, the male trait (body size) is inherited from both parents[9], but whether the female preference itself is genetically variable and a correlate of the male trait was unknown.

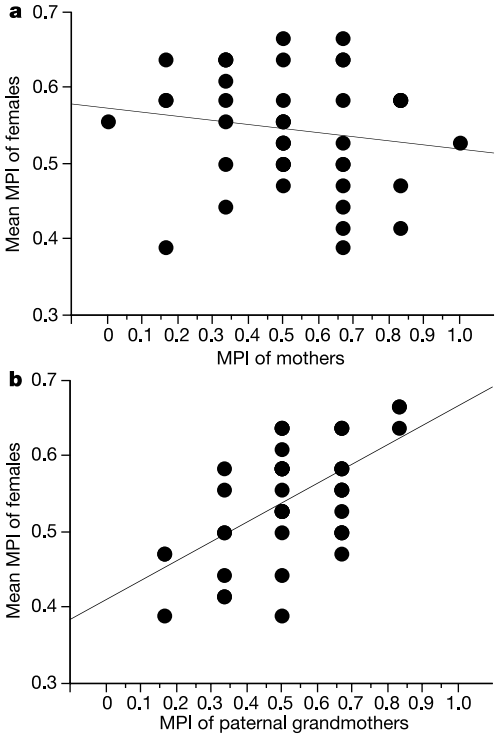


**Figure 1** Mean mating preference index (MPI) of females (six full sisters) plotted as a function of the mating preference index of their mother and paternal grandmother ($n = 44$). **a**, The MPI values of females and their mothers are not correlated ($r^2 = 0.025$, $P = 0.305$, $y = 0.574 - 0.054x$), indicating that the mating preference is not inherited via the mother. **b**, The MPI values of females and their paternal grandmothers are positively correlated ($r^2 = 0.333$, $P < 0.0001$, $y = 0.41 + 0.257x$), indicating that the mating preference is paternally inherited by daughters [$h^2 = 0.513 \pm 0.112$ (mean $\pm$ s.e.)].


© 2002 Nature Publishing Group

Received 22 November; accepted 23 December 2002; doi:10.1038/nature01378.
Published online 22 January 2003.

1. Grunstein, M. Histone acetylation in chromatin structure and transcription. *Nature* **389,** 349–352 (1997).
2. Turner, B. M. Histone acetylation and an epigenetic code. *Bioessays* **22,** 836–845 (2000).
3. Berger, S. L. Histone modifications in transcriptional regulation. *Curr. Opin. Genet. Dev.* **12,** 142–148 (2002).
4. Lachner, M. & Jenuwein, T. The many faces of histone lysine methylation. *Curr. Opin. Cell Biol.* **14,** 286–298 (2002).
5. Strahl, B. D. & Allis, C. D. The language of covalent histone modifications. *Nature* **403,** 41–45 (2000).
6. Zhang, X. *et al.* Structure of the neurospora SET domain protein DIM-5, a histone H3 lysine methyltransferase. *Cell* **111,** 117–127 (2002).
7. Spotswood, H. T. & Turner, B. M. An increasingly complex code. *J. Clin. Invest.* **110,** 577–582 (2002).
8. Feng, Q. *et al.* Methylation of H3-lysine 79 is mediated by a new family of HMTases without a SET domain. *Curr. Biol.* **12,** 1052–1058 (2002).
9. van Leeuwen, F., Gafken, P. R. & Gottschling, D. E. Dit1p modulates silencing in yeast by methylation of the nucleosome core. *Cell* **109,** 745–756 (2002).
10. Jenuwein, T. Re-SET-ting heterochromatin by histone methyltransferases. *Trends Cell Biol.* **11,** 266–273 (2001).
11. Wilson, J. R. *et al.* Crystal structure and functional analysis of the histone methyltransferase SET7/9. *Cell* **111,** 105–115 (2002).
12. Jacobs, S. A. *et al.* The active site of the SET domain is constructed on a knot. *Nature Struct. Biol.* **9,** 833–838 (2002).
13. Trievel, R. C., Beach, B. M., Dirk, L. M. A., Houtz, R. L. & Hurley, J. H. Structure and catalytic mechanism of a SET domain protein methyltransferase. *Cell* **111,** 91–103 (2002).
14. Min, J., Zhang, X., Cheng, X., Grewal, S. I. & Xu, R. M. Structure of the SET domain histone lysine methyltransferase Clr4. *Nature Struct. Biol.* **9,** 828–832 (2002).
15. Santos-Rosa, H. *et al.* Active genes are tri-methylated at K4 of histone H3. *Nature* **419,** 407–411 (2002).
16. Rea, S. *et al.* Regulation of chromatin structure by site-specific histone H3 methyltransferases. *Nature* **406,** 593–599 (2000).
17. Hofmann, J. L. Chromatographic analysis of the chiral and covalent instability of *S*-adenosyl-L-methionine. *Biochemistry* **25,** 4444–4449 (1986).
18. Otwinowski, Z. & Minor, W. in *Data Collection and Processing* (eds Sawyer, L., Isaacs, N. & Bailey, S.) 556–562 (SERC Daresbury Laboratory, Warrington, 1993).
19. CCP4. The CCP4 suite: programs for protein crystallography. *Acta Crystallogr. D* **50,** 760–763 (1994).
20. Jones, T. A., Zhou, J. Y., Cowan, S. W. & Kjeldgaard, M. Improved methods for building protein models in electron density maps and the location of errors in these models. *Acta Crystallogr. A* **47,** 110–119 (1991).

**Supplementary Information** accompanies the paper on *Nature*'s website (http://www.nature.com/nature).

**Acknowledgements** We are grateful to G. Dodson and S. Smerdon for critical reading of the manuscript, and to Y. Shinkai and Y. Tanaka for the gift of the G9a clone. NMR spectra were recorded at the MRC Biomedical NMR Centre.

**Competing interests statement** The authors declare that they have no competing financial interests.

**Correspondence** and requests for materials should be addressed to S.J.G. (e-mail: sgambli@nimr.mrc.ac.uk). Coordinates for the SET7/9 ternary complex have been deposited with the Protein Data Bank under accession code 1o9s.

## corrigendum

# Contemporary fisherian life-history evolution in small salmonid populations

**Mikko T. Koskinen, Thrond O. Haugen & Craig R. Primmer**

*Nature* **419**, 826–830 (2002).

The neutrality test equation applied in this Letter ($F = (N_e\sigma^2_{GB})/(h^2\sigma^2_{GW}t)$) was incorrect: the correct equation is $F = (N_e\sigma^2_{GB})/(\sigma^2_{GW}t)$. Consequently, the numbers in the right three columns of the original Table 1 are wrong (corrected below). In addition, some variance estimates in Table 1 and some values of Fig. 2 were reported incorrectly (the entire correct Table 1 and the correct Fig. 2 are available from the authors). These errors do not affect our conclusion that the populations evolved predominantly as a result of natural selection. We thank W. G. Hill for bringing these errors to our attention. □

Table 1

| Trait | Pairwise comparison | $F_{1,\infty}$ | $P$ | $N_e$ (sign) |
|---|---|---|---|---|
| Length at termination (mm) | Les–Ht | 37.7 | *** | 2.5 |
| | Les–Aur | 0.78 | 0.38 | 272 |
| | Ht–Aur | 8.63 | ** | 17.7 |
| Yolk-sac volume ($mm^3$) | Les–Ht | 29.0 | *** | 3.21 |
| | Les–Aur | 59.2 | *** | 3.59 |
| | Ht–Aur | 3.17 | 0.07 | 48.3 |
| Growth rate ($mm/\Delta D$) | Les–Ht | 20.5 | *** | 4.55 |
| | Les–Aur | 6.31 | ** | 33.7 |
| | Ht–Aur | 41.5 | *** | 3.68 |
| Survival (%) | Les–Ht | 5.90 | * | 15.8 |
| | Les–Aur | 3.13 | 0.08 | 68.0 |
| | Ht–Aur | 1.20 | 0.27 | 128 |
| Incubation time (days) | Les–Ht | 4.02 | * | 23.1 |
| | Les–Aur | $1.56 \times 10^{-7}$ | >0.99 | $1.36 \times 10^{9}$ |
| | Ht–Aur | 7.82 | ** | 19.5 |
| Swim-up length (mm) | Les–Ht | 0.26 | 0.61 | 363 |
| | Les–Aur | 0.04 | 0.84 | $5.79 \times 10^{3}$ |
| | Ht–Aur | $2.73 \times 10^{-8}$ | >0.99 | $5.60 \times 10^{9}$ |
| Hatching length (mm) | Les–Ht | $1.46 \times 10^{-8}$ | >0.99 | $6.38 \times 10^{9}$ |
| | Les–Aur | 0.78 | 0.38 | 274 |
| | Ht–Aur | $2.16 \times 10^{-8}$ | >0.99 | $7.07 \times 10^{9}$ |

 © 2003 Nature Publishing Group 